International Conference on Renewable Energies and Power Quality (ICREPQ'17)
Malaga (Spain), 4th to 6th April, 2017
Renewable Energy and Power Quality Journal (RE&PQJ)
ISSN 2172-038 X, No.15 April 2017

A Fixed-Frequency Soft-Switched Interleaved 3-Phase AC-to-DC Converter

Y. Du[2] and A.K.S. Bhat[1*]

[1*] (Corresponding author) Department of Electrical and Computer Engineering
University of Victoria
Victoria, BC, V8W 3P6 (Canada)
Phone number: 1-250-721-8682, e-mail: abhat@engr.uvic.ca

[2] Is now with Rinte pipe Ecomaterial Co., Ltd., Chang Zhou, 213000, China (email: du.yimian@rintepipe.com).

Abstract: This paper proposes a three-phase interleaved high-frequency transformer isolated ac-dc converter that is suitable for small scale wind energy conversion systems employing permanent magnet synchronous generators. This configuration is realized by interleaving three identical single-phase single-stage ac-dc converters obtained by integrating a rectifier, boost converter and fixed-frequency dual-tank LCL resonant converters. Based on a design example used for illustration purpose, a converter is designed and PSIM simulation results are presented for various operating conditions, such as balanced and unbalanced 3-phase operation; two-phase operation. It is shown that the converter maintains soft switching fore wide variation in supply voltage with low THD with high power factor.
.

Key words

Interleaved, soft-switched, PMSG, power factor correction, ac-to-dc.

1. Introduction

AC-to-DC controlled rectifiers are used widely in power supplies for various applications and in energy systems. Direct-driven permanent magnet synchronous generators (PMSG) are becoming more attractive for wind energy generation system especially in small scale applications (up to about 12 kW) such as residential purpose due to easy installation and low price, e.g. [1]. Not only the generator gives high efficiency because of removing magnetizing field excitation circuit, mechanical component is also reduced such as the absence of slip rings, which increases the system reliability and the ratio of power to weight. Power electronic converters are used in wind energy conversion system (WECS) to transfer the variable-amplitude variable-frequency (VAVF) ac output from the wind turbine driven PMSG to desired grid ac voltage and frequency. Power converters used in WECS consist of two parts: front-end ac-dc rectifier which is used to convert VAVF ac voltage to dc bus voltage followed by an inverter. Most of the WECS choose line frequency (LF) isolated transformer placed between the dc-ac inverter and the grid, e.g., [2]-[10]. Some of these systems use diode rectifiers to get uncontrolled dc output from the generator [2]-[6], whereas, use of controlled rectifiers is reported in [7]-[10]. Use of uncontrolled diode rectifier [2]-[6] will cause higher armature currents due to current harmonics decreasing the generator efficiency. Use of controlled rectifiers can achieve high power factor with low harmonic distortion will improve the overall efficiency of such systems [7]-[10]. There are limited reports about high-frequency (HF) transformer isolated ac-dc converter used for WECS in the literature, e.g., [11-12]. Here HF refers to operation frequency above 20 to 50 kHz. Compared to LF isolated transformer, HF transformer isolation has many advantages such as small size, low cost, and easy integration with converter. Fixed-frequency variable voltage source is assumed in [11] while VAVF operation is possible in [12].

Fig. 1 shows the single-phase single-stage ac-dc converter utilizing an integrated dual-tank LCL-type series resonant proposed in [12]. A fixed frequency phase-shift control technique was used for output voltage regulation. This dual-tank LCL ac-dc converter achieves a high power factor and low ac input current THD at the ac input side. It still includes expected HF isolation, power factor correction (PFC), and output voltage regulation in one single-stage. Soft-switching operation is guaranteed in the entire operating range. Objectives of this paper are to extend its use in a 3-phase conversion that can be used in a small scale wind energy conversion systems (but can also be used in other ac-dc power supply applications), then to design and simulate the proposed converter to evaluate its performance. These objectives are realized in different sections as follows: The proposed three-phase interleaved ac-dc converter including three identical dual-tank LCL-type series ac-dc converters is presented in Section 2. The circuit description and operation will also be briefly presented here. A design example is presented in Section 3. PSIM simulation results for various operating conditions to evaluate the performance of the designed converter are given in Section 4. Section 5 presents the conclusions.

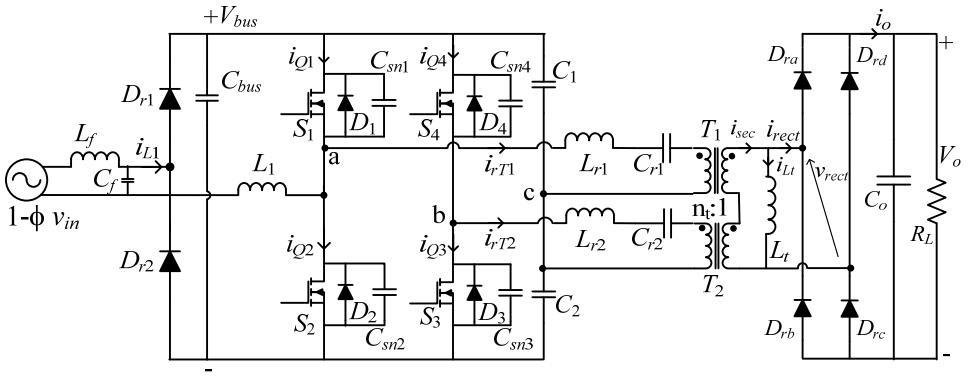

Fig. 1 Single-phase, single-stage ac-to-dc dual-tank LCL resonant soft-switched converter [12].

2. Proposed Converter Description and Operation

In the proposed single-phase configuration (Fig. 1) [12], a dual-switch boost converter (D_{r1}, D_{r2}, S_1, S_2, L_1) is integrated with a half-bridge resonant converter (S_1, S_2, C_1, C_2, L_{r1}, C_{r1}, T_1). The other half-bridge resonant converter (S_3, S_4, C_1, C_2, L_{r2}, C_{r2}, T_2) shares the dc bus capacitor (C_{bus}) with the first half-bridge converter. Two identical HF transformers (T_1, T_2) are connected in series on secondary-side to form a dual-tank configuration. An external inductor (L_t) is connected in parallel with the terminal of secondary-side of T_1/T_2 to achieve LCL-type series resonant circuit. The magnetizing inductances of each transformer can be considered as parts of the paralleled inductor. A high PF and low THD are achieved by discontinuous current mode (DCM) operation in L_1 over the entire line frequency cycle at the ac input side. Since T_1 and T_2 are connected in series on secondary-side, i_{rT1} and i_{rT2} are always identical ($i_{rT1} = i_{rT2}$).

Fig. 2 shows a Y-connected three-phase interleaved configuration scheme used for three-phase application. As can be seen, each single-phase converter handles a single-phase output. The dc output of each single-phase converter is connected in parallel so that the combined output voltage is the same as single-phase circuit output, but the output power is three times of the single-phase output and the ripple frequency will be higher. The power generated by PMSG can be transferred to the load or the grid through three identical paths, so the components stresses of each single-phase converter are reduced. Operation of each single-phase converter is independent, but gating signals need to be phase-shifted by 120° between each other. The operation of each single-phase converter has been illustrated in [12], and is not repeated here. The power factor and THD at the input side remains the same as those used for single-phase input. Main advantages of interleaved configuration are: (a) the total power is transferred through three identical paths, so power components stresses are reduced; (b) distribution of thermal stresses; (c) such a configuration still works under an unbalance input condition, i.e., if amplitudes of phases are different or if one or two phase inputs fail, the other one can still work; (d) easy to replace a module in case of any failure.

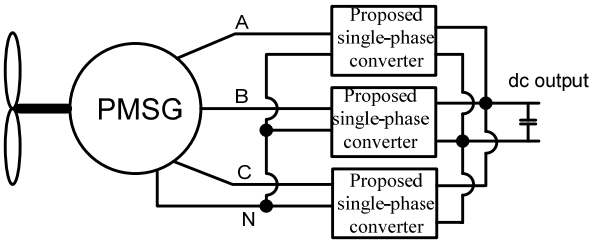

Fig. 2 Three-phase ac-to-dc converter realized by using interleaved connection of three single-phase converter of Fig. 1.

3. Design Example

To illustrate design procedure, a low power 3-ϕ design example is given with the values: Input voltage (line-to neutral, peak value) $\sqrt{2}V_{in}$: 60 V, 40 Hz to 80 V, 60 Hz (e.g., in a WECS); output power, P_o = 300 W; and dc output voltage, V_o = 100 V. Switching frequency is 100 kHz. Design procedure steps are the same as given in [12] and are summarized below:
(a) Front-end dual-switch boost converter part, the boost inductor L_1 for DCM operation is determined by the minimum ac input voltage and the value obtained is L_1 = 40 μH. (b) The LCL converter is designed at the minimum ac input voltage, and the optimal design parameters are chosen as (based on design curves given in [12]): switching frequency ratio, F = 1.1; normalized load current, J = 0.5; converter gain, M_f = 0.955; and the base voltage, V_B = 120V. Load resistance corresponding to power supplied by each module, $R_L = V_o^2/P_o = 100\ \Omega$, $I_o = V_o/R_L = 1$ A, $V'_o = M_f V_B = 114.6$V, $n_t = V'_o/V_o = 1.146$. The resonant inductance and capacitance for each module can be calculated as [12]-[13]:

$$L_{r1} = L_{r2} = \frac{1}{2}\left(\frac{M_f V_B^2 JF}{2\pi f_s P}\right) = 60.2\ \mu H$$

$$C_{r1} = C_{r2} = 2\left(\frac{PF}{2\pi f_s M_f V_B^2 J}\right) = 50.9\ nF$$

Parallel resonant inductance (including magnetizing inductance of HF transformers) referred to secondary side is L_p = 923 μH (for a ratio of primary-side L_p/L_r = 20). The load resistance is R_L = 33.3 Ω for 300 W output.

4. Simulation Results

The proposed three-phase interleaved circuit is simulated using PSIM simulation package. The generated gating signals are such that three groups of complementary gating signals have 120° of phase-shift between each phase in order to match 3-ϕ application operation. In this example, two groups of simulated results are obtained based on both balanced and unbalance ac input, respectively. One phase voltage with 90% of amplitude is used to demonstrate the proposed circuit operation for the unbalanced input condition.

A. Balanced AC Input

Since PMSG provides a balanced 3-ϕ output, two different input voltages are applied to the proposed 3-ϕ interleaved circuit for simulation. When $\sqrt{2}V_{in}$ = 60 V, 40 Hz and phase-shift (θ) between LCC modules is θ = 0, the ac input voltage and current, the corresponding FFT of the ac input current, and boost inductor current are captured, shown in Fig 3. The tank HF key voltages and currents are shown in Fig. 4. In Fig. 3(a) and Fig. 3(b), a 0.99 of power factor and 10% of THD are obtained for each phase. The boost current is in DCM as shown in Fig. 3(c). The output voltage ripple (97 to 100.5 V, peak-to-peak) is shown in Fig 3(d). The HF tank inverting voltage (v_{ab}) and resonant current (i_{rT1}), and HF diode rectifier input voltage (v_{rect}) and current (i_{rect}) for each phase are shown in Fig. 4. Fig. 4(a) shows lagging resonant current nature proving zero-voltage switching (ZVS) operation for the switches. Fig. 4(b) shows that resonant converter rectifier voltage is clamped at the output voltage. All waveforms for each phase are identical and 120° of phase-shifted by each other, which agrees with the theory.

When $\sqrt{2}V_{in}$= 80 V, 60 Hz, θ = 108°, the ac input voltage and current, the corresponding FFT of the ac input current, and boost inductor current are shown in Fig 5. Several key HF tank voltages and currents are shown in Fig. 6. A unity of power factor and 12.5% of THD are obtained based on Fig. 5(a) and (b) for each phase. The boost current is still in DCM (Fig. 5(c)). The output voltage ripple (97.55 to 97.72 V, peak-to-peak) is shown in Fig 5(d). The key HF waveforms on primary-side, and secondary-side of HF transformers are shown in Figs. 6(a) and 6(b), respectively for each phase. Based on waveforms obtained, all waveforms for each phase are identical and 120° of phase-shifted by each other, which also agrees with the theory.

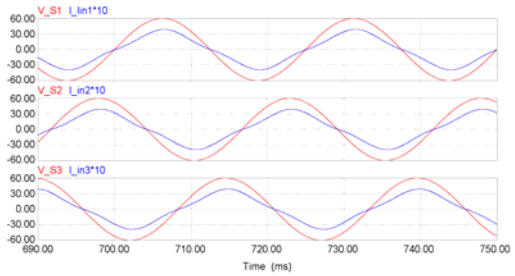

Fig. 3(a)

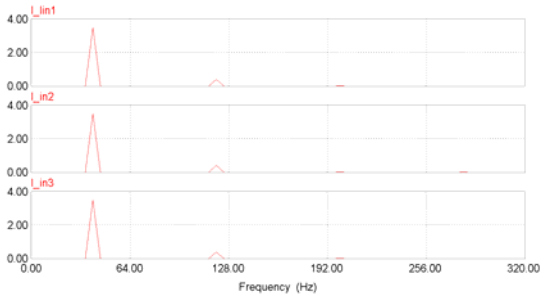

(b)

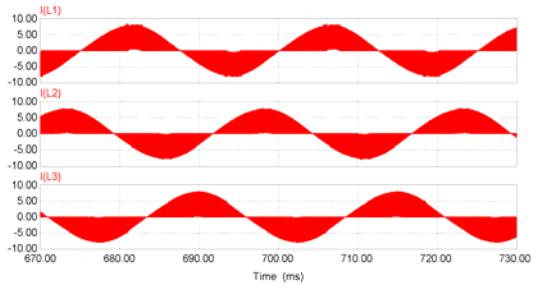

(c)

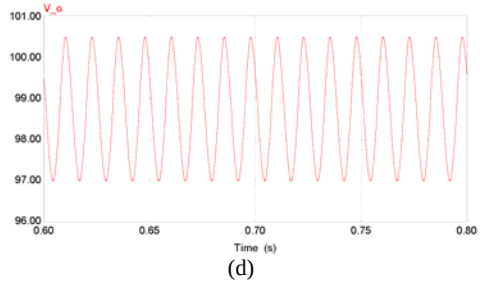

(d)

Fig. 3 Balanced input condition at$\sqrt{2}V_{in}$ = 60 V, 40 Hz, θ = 0: (a) ac input voltage and current in each phase; (b) FFT spectrum of ac input current; (c) boost current for each single-phase converter, for each phase; (d) output voltage ripple.

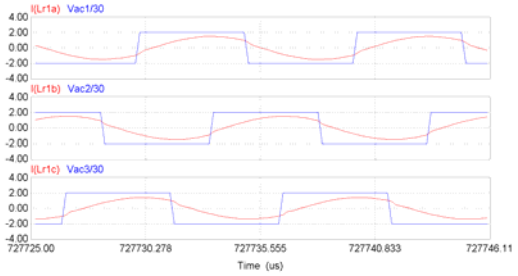

(a)

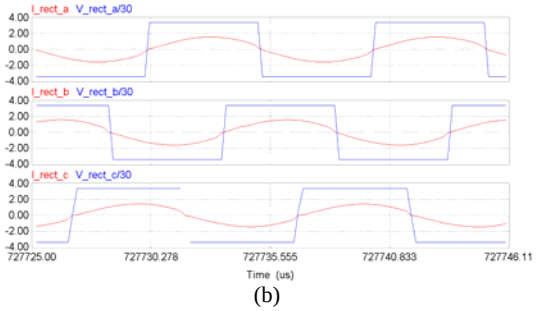

(b)

Fig. 4 Balanced input condition at $\sqrt{2}V_{in}$ = 60 V, 40 Hz, θ = 0: (a) HF tank inverting input voltage (v_{ab}) and tank resonant current (i_{rT1}); (b) HF diode rectifier input voltage (v_{rect}) and current (i_{rect}), for each phase circuit.

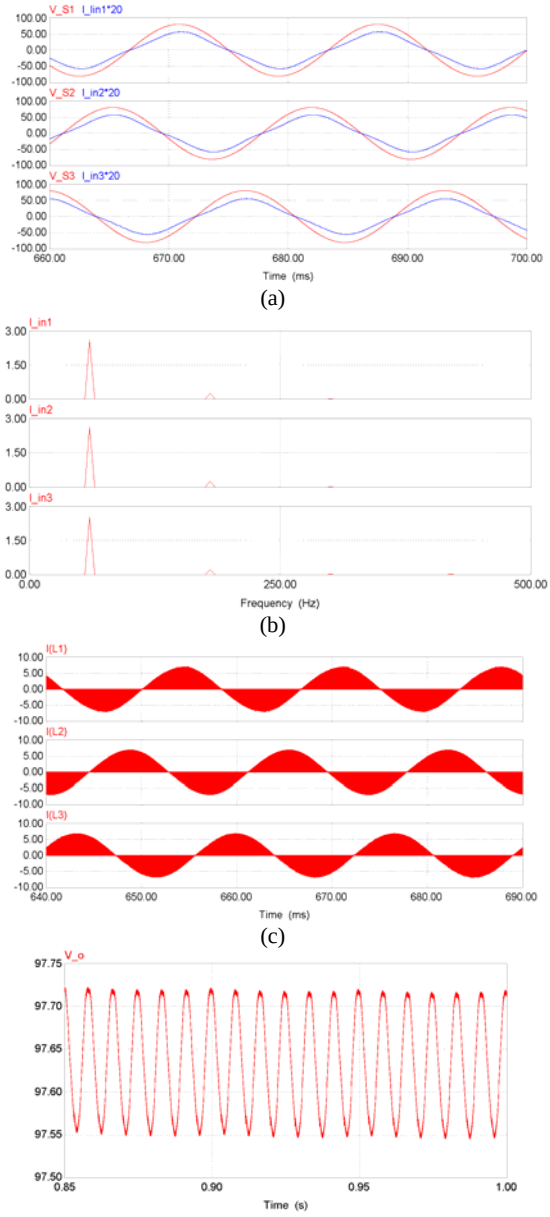

Fig. 5 Balanced input condition at $\sqrt{2}V_{in}$ = 80 V, 60 Hz, θ = 108°: (a) ac input voltage and current in each phase; (b) FFT spectrum of ac input current; (c) boost current for each single-phase converter for each phase; (d) output voltage ripple.

B. Unbalanced AC Input

For an unbalanced 3-ϕ input from PMSG, such as Phase A with 90% of amplitude (54 V, 72V) and the other two phases with 100% of amplitude (60 V, 80V). Two different input voltages ($\sqrt{2}V_{in,min}$ = 60 V and $\sqrt{2}V_{in,max}$ = 80 V, peak value of line-to-neutral) are also applied to the proposed three-phase circuit, shown in Fig. 7 and Fig. 8, respectively. The ac input voltages and currents of the interleaved 3-ϕ ac-dc converter are shown in Fig. 7(a) and Fig. 8(a), and the corresponding FFT spectrum of the ac input current are given in Fig. 7(b) and Fig. 8(b). According to Fig. 7(b), when $\sqrt{2}V_{in}$ = 60 V, 40 Hz, we obtain 10% of THD at phase A, and 12.5% of THD at phase B and phase C. The dc output voltage ripple is

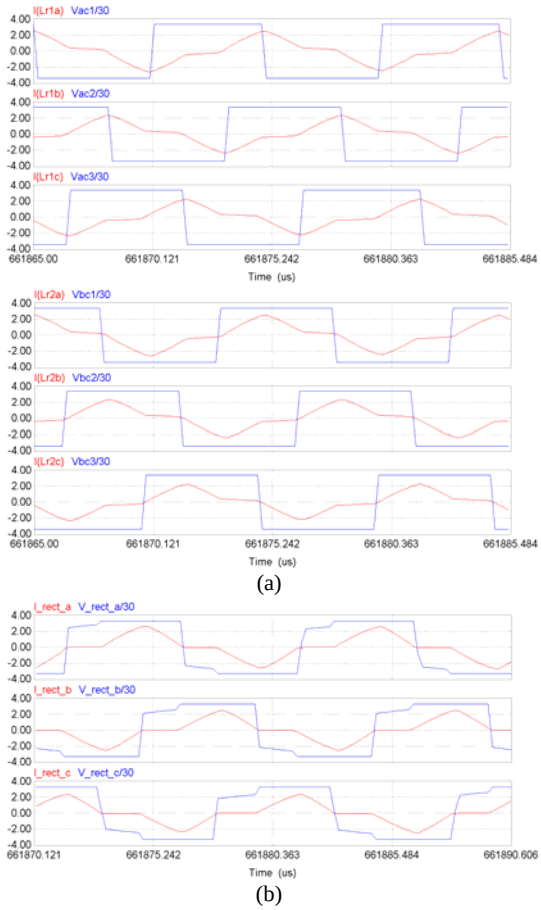

Fig. 6 Balanced input condition at $\sqrt{2}V_{in}$ = 80 V, 60 Hz, θ = 108°: (a) HF tank inverting input voltages (v_{ab}, v_{bc}) and tank resonant current (i_{rT1}, i_{rT2}); (b) HF diode rectifier input voltage (v_{rect}) and current (i_{rect}), for each phase circuit.

shown as Fig. 7(c). The peak-to-peak voltage ripple is about 91.5 to 97.5 V. In Fig. 8(b), when $\sqrt{2}V_{in}$ = 80 V, 60 Hz, we also obtain 8.5% of THD at phase A, and 9% of THD at phase B and phase C. The dc output voltage ripple is shown as Fig. 8(c). The peak-to-peak voltage ripple is about 88 to 94 V.

Table 1 summaries input current THD under unbalanced input voltage condition. Based on values in this table, the proposed three-phase interleaved ac-dc converter brings low input current THD for each phase, even under unbalanced input voltage condition.

TABLE 1 Unbalanced inputs for three-phase interleaved ac-dc converter

(90% of amplitude in Phase A, 100% of amplitude in Phase B and Phase C)			
	Phase A	Phase B	Phase C
$\sqrt{2}V_{in}$ = 60 V	54V	60V	60V
$\sqrt{2}V_{in}$ = 80 V	72V	80V	80V
THD at $\sqrt{2}V_{in}$ = 60 V	10%	12.5%	12.5%
THD at $\sqrt{2}V_{in}$ = 80 V	8.5%	9%	9%

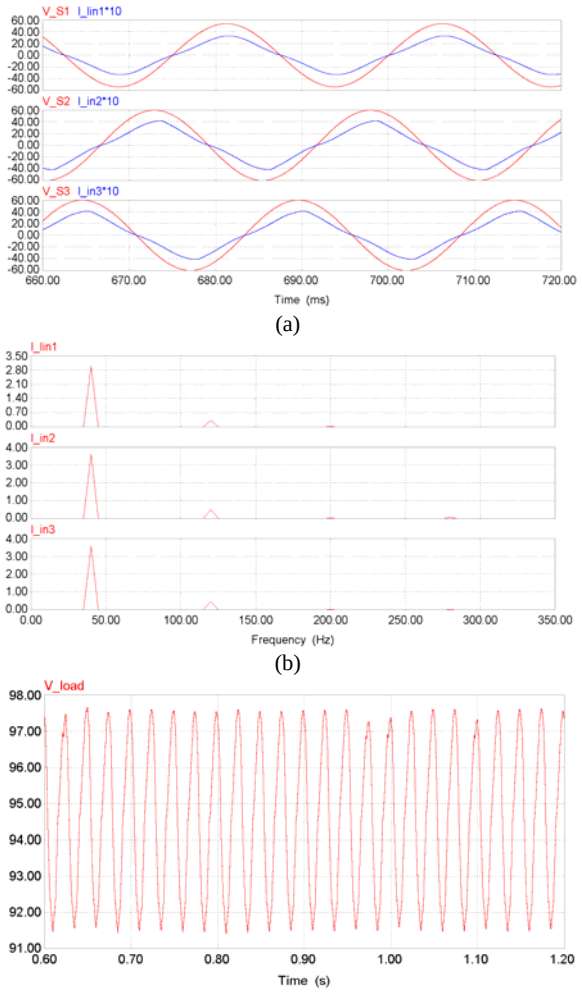

Fig. 7 Unbalance input condition($\sqrt{2}V_{in,min}$ = 60 V): (a) ac input voltage and current in each phase (90% of amplitude in phase A); (b) FFT spectrum of ac input current; (c) output voltage ripple.

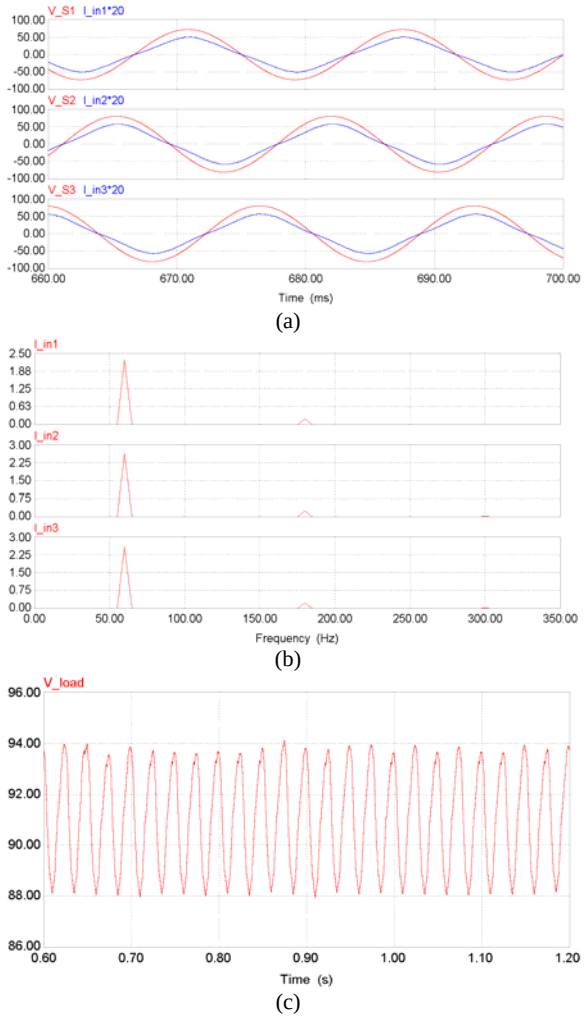

Fig. 8 Unbalance input condition($\sqrt{2}V_{in,max}$ = 80 V): (a) ac input voltage and current in each phase (90% of amplitude in phase A); (b) FFT spectrum of ac input current; (c) output voltage ripple.

C. Two-Phase Operation

In this section, some simulated results show the 300 W of three-phase interleaved circuit operating under two-phase operation (i.e., one phase circuit fails). Two different input voltages ($\sqrt{2}\boldsymbol{V_{in,min}}$ = 60 V and $\sqrt{2}\boldsymbol{V_{in,max}}$ = 80 V) are also applied to the proposed three-phase circuit, shown in Fig. 9 and Fig. 10, respectively. The ac input voltages and currents of the interleaved three-phase ac-dc converter are shown in Fig. 9(a) and Fig. 10(a), and the corresponding FFT spectrum of the ac input current are given in Fig. 9(b) and Fig. 10(b). According to Fig. 9(b), when $\sqrt{2}\boldsymbol{V_{in}}$ = 60 V, 40 Hz, we obtain 25% of THD at each phase. The dc output voltage ripple is shown as Fig. 9(c). The peak-to-peak voltage ripple is about 90.25 to 93.25 V. In Fig. 10(b), when $\sqrt{2}\boldsymbol{V_{in}}$ = 80 V, 60 Hz, we also obtain 10% of THD for each phase. The dc output voltage ripple is shown as Fig. 10(c). The peak-to-peak voltage ripple is about 81.7 to 82.5 V. Since each sing-phase converter work independently, the HF waveforms will not change in two-phase operating condition, and they will not be repeated here.

5. Conclusion

In this paper, a three-phase interleaved ac-dc converter is proposed for PMSG-based wind generation system. Three identical single-stage dual-tank LCL-type series resonant ac-dc converters are connected as the proposed three-phase interleaved configuration circuit. The proposed interleaved configuration is recommended for PMSG based WECS and other ac-to-dc applications. A design example and simulation are given to show performances of the interleaved configuration for various operating conditions. This configuration brings a high power factor and low line-current THD at the ac input side under the balanced ac input, full-load condition. If amplitudes of phases are different or if one or two phase inputs fail, the performances of the three-phase interleaved configuration are still acceptable even though ac input current THD increases from 10% to 24%. This converter maintains ZVS for all the switches. Future work will concentrate on implementing an experimental converter to verify the performance and also to reduce the THD further.

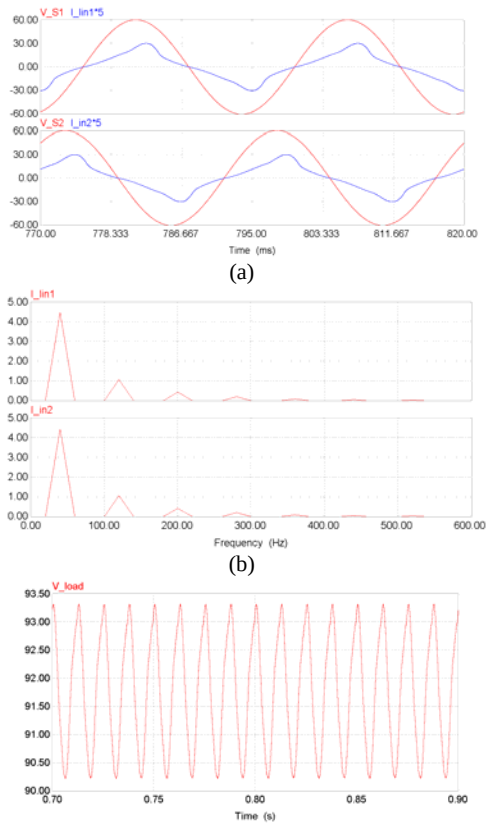

Fig. 9 Two-phase operation at $\sqrt{2}V_{in}$ = 60 V, 40 Hz: (a) ac input voltage and current in two phases (Phase C fails); (b) FFT spectrum of ac input current; (c) output voltage ripple.

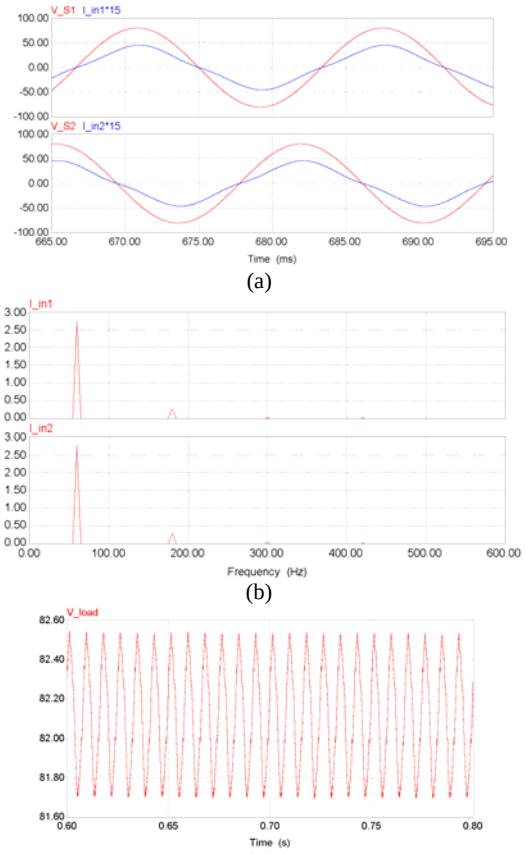

Fig. 10 Two-phase operation at $\sqrt{2}V_{in}$ = 80 V, 60 Hz: (a) ac input voltage and current in two phases (Phase C fails); (b) FFT spectrum of ac input current; (c) output voltage ripple.

Acknowledgement

This work was supported by a research grant from the Natural Sciences and Research Council of Canada.

References

[1] XZERES Wind. "Xzeres wind product". Website, May 2011. http://www.xzeres.com/products/.

[2] Z. Chen and E. Spooner. "Voltage source inverters for high-power, variable-voltage DC power sources," *Generation, Transmission and Distribution, IEE Proceedings, IET*, vol. 148, pp. 439–447, 2001.

[3] S.M. Dehghan, M. Mohamadian, and A.Y. Varjani. "A new variable-speed wind energy conversion system using permanent-magnet synchronous generator and Z-source inverter," *IEEE Trans. on, Energy Conversion*, vol. 24, no. 3, pp. 714–724, 2009.

[4] D.M. Vilathgamuwa, W. Xiaoyu, and CJ Gajanayake. "Z-source converter based grid-interface for variable-speed permanent magnet wind turbine generators," *in PESC 2008. IEEE*, pp. 4545–4550, 2008.

[5] F. Deng and Z. Chen. "Power control of permanent magnet generator based variable speed wind turbines," *in ICEMS 2009, IEEE*, pp.1–6, 2009.

[6] M.E. Haque, M. Negnevitsky, and K.M. Muttaqi. "A novel control strategy for a variable-speed wind turbine with a permanent-magnet synchronous generator," *IEEE Trans. on, Industry Applications*, vol. 46, no. 1, pp. 331–339, 2010.

[7] D.S. Oliveira, M.M. Reis, C. Silva, C. Barreto, F. Antunes, and B.L. Soares. "A three-phase high-frequency semi-controlled rectifier for PM WECS," *IEEE Trans. on, Power Electronics*, vol. 25, no. 3, pp. 677–685, 2010.

[8] M. Singh, V. Khadkikar, and A. Chandra. "Grid synchronization with harmonics and reactive power compensation capability of a permanent magnet synchronous generator-based variable speed wind energy conversion system," *IET, Power Electronics*, vol. 4, no.1, pp. 122–130, 2011.

[9] D.C. Lee and D.S. Lim. "AC voltage and current sensorless control of three-phase PWM rectifiers," *IEEE Trans. on, Power Electronics*, vol. 17, no. 6, pp. 883–890, 2002.

[10] T. Kominami and Y. Fujimoto. "A novel nine-switch inverter for independent control of two three-phase loads," *in IAS 2007, IEEE*, pp. 2346–2350, 2007.

[11] H.J. Chua and P.N. Enjeti, A three-phase AC/AC high-frequency link matrix converter for VSCF applications," in *IEEE PESC*, 2003, pp. 1971-1976.

[12] Y. Du and A.K.S. Bhat, "Analysis and design of a high-frequency isolated dual-tank LCL resonant AC-DC converter", *IEEE Internatl. Power Electronics Conf., ECCE Asia*,Hiroshima, Japan, pp. 1721-1727, May 18-21, 2014.

[13] Y. Du, "A high-frequency isolated integrated resonant ac-dc converters for PMSG based wind energy conversion system," *Ph.D. Dissertation*, Dept. of ECE, University of Victoria, B.C., 2013.